

Supporting Information

Two-Dimensional Active Surface Growth in Ag Nanoplates

Jin Ji,^{1,2} Zijie Chen,¹ Tingting Jiang,¹ Yuhua Feng,^{1,*} and Hongyu Chen^{2,3,*}

1. Institute of Advanced Synthesis (IAS), School of Chemistry and Molecular Engineering, Jiangsu National Synergetic Innovation Centre for Advanced Materials, Nanjing Tech University, Nanjing, 2118816, China.

2. Department of Chemistry, School of Science and Research Center for Industries of the Future, Westlake University, 600 Dunny Road, Hangzhou 310030, Zhejiang Province, China.

3. Institute of Natural Sciences, Westlake Institute for Advanced Study, 18 Shilongshan Road, Hangzhou 310024, Zhejiang Province, China.

**Corresponding author:*

**Hongyu Chen, chenhongyu@westlake.edu.cn;*

**Yuhua Feng, ias_yhfeng@njtech.edu.cn*

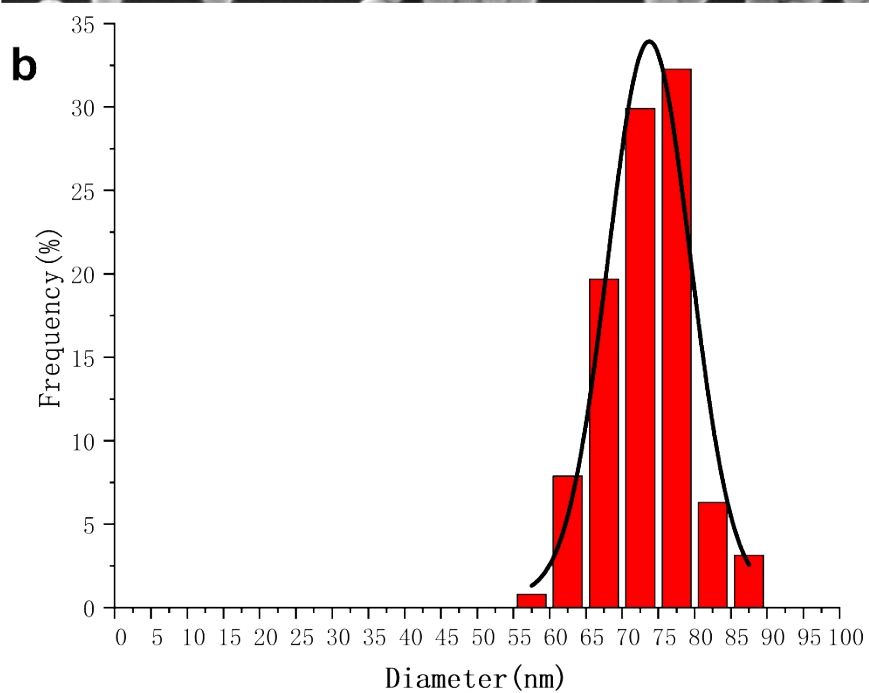
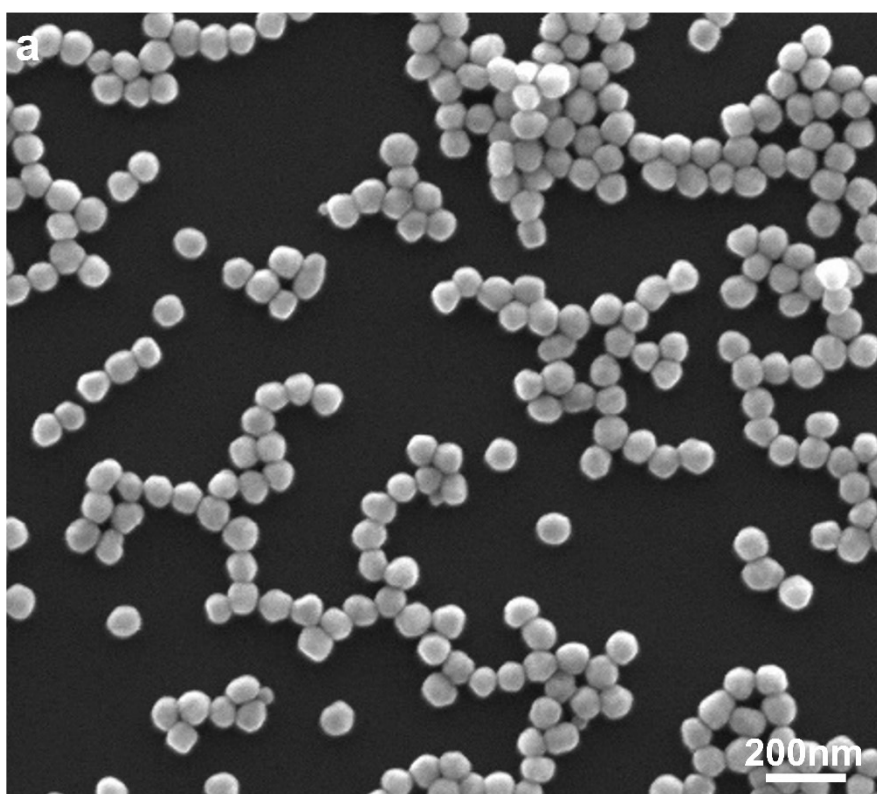


Fig. S1. (a) TEM image and (b) diameter distribution of 70 nm Au seeds.

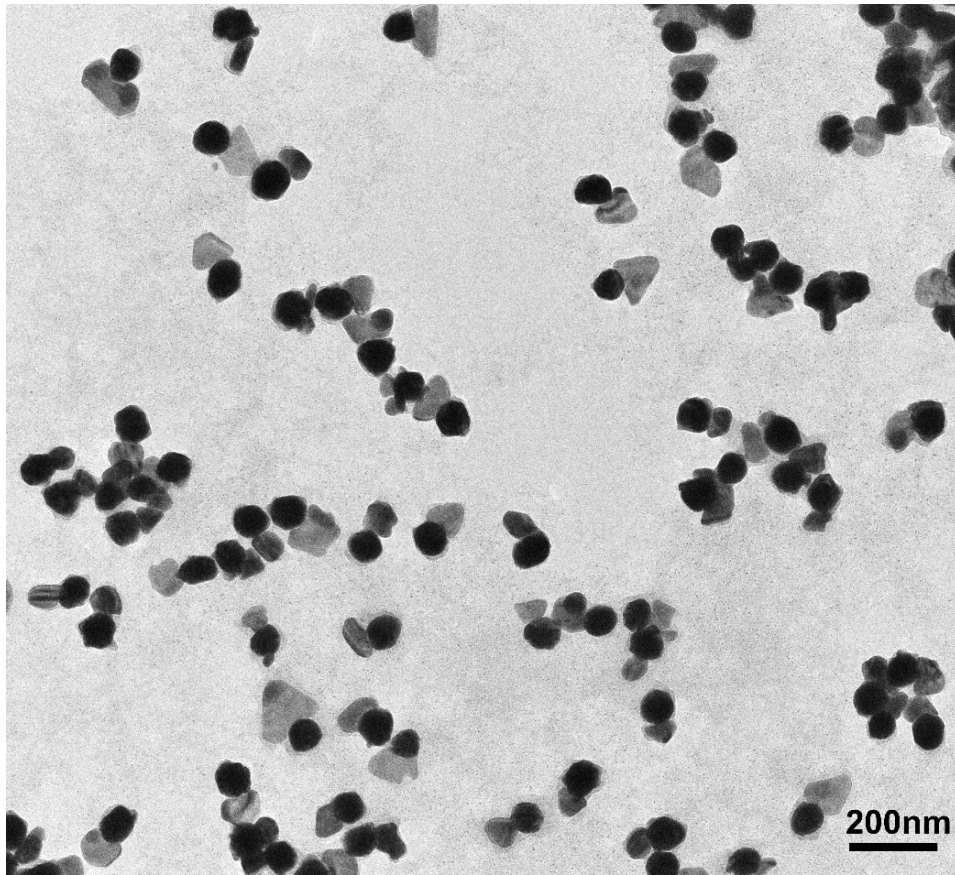


Fig. S2. TEM image of Au-Ag plate dimer structure similar to that in Fig. 1b without PSPAA encapsulation.

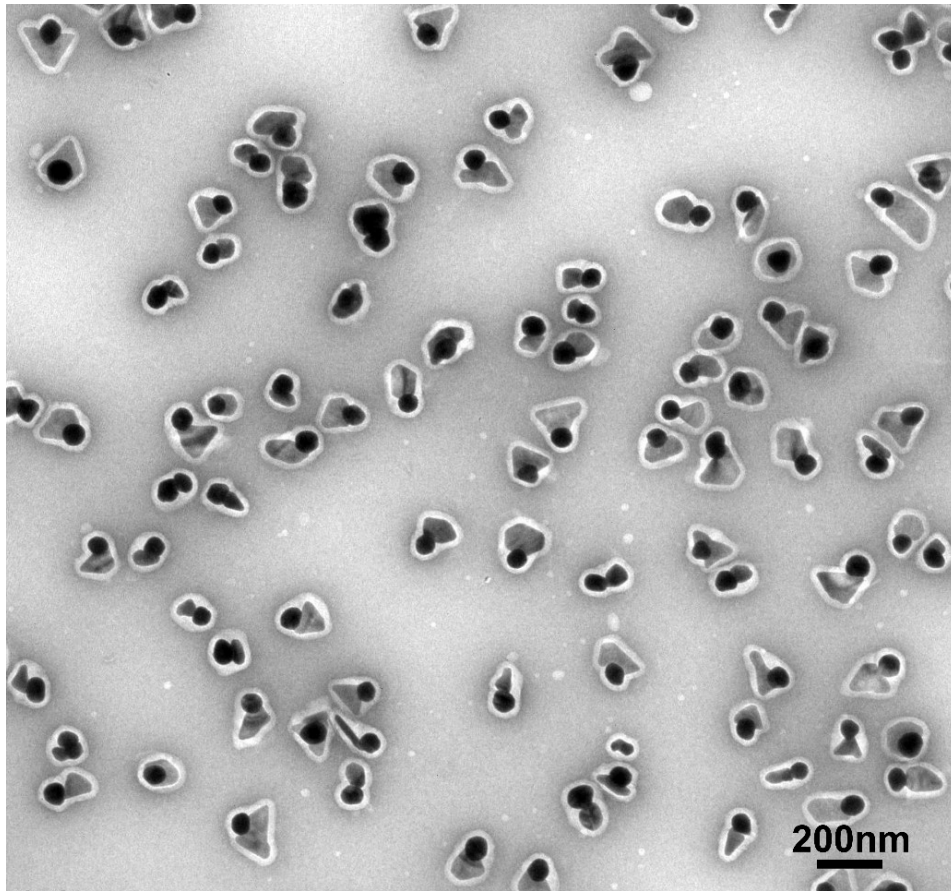


Fig. S3. TEM image of Au-Ag plate hybrid structure used for the purity survey: among the 104 nanoparticles, 99 are Au sphere-Ag plate dimers.

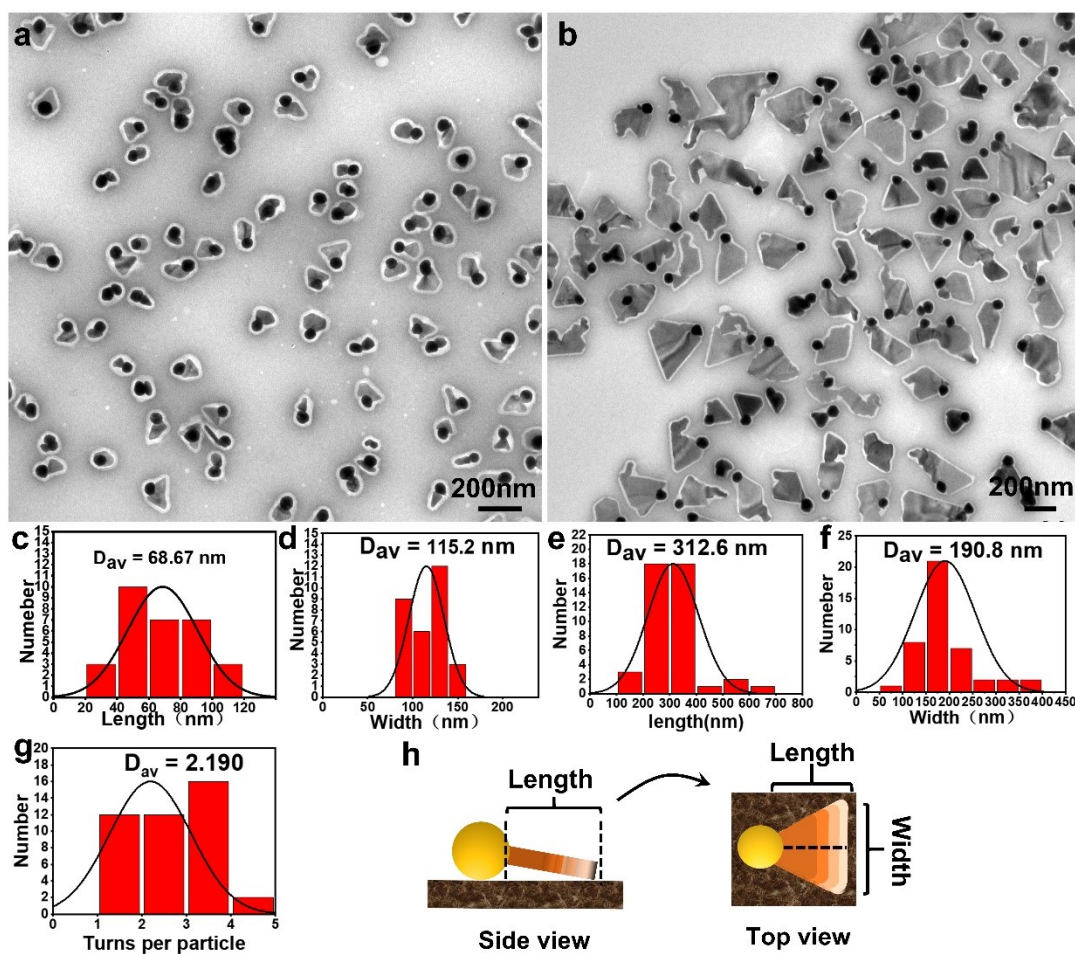


Fig. S4. TEM images of the (a) Au-Ag triangle plate and (b) Au-Ag plate heterostructures. The statistic distribution of the (c) length and (d) width of the Ag nanoplates in Au-Ag triangle plate and (e) length and (f) width of the Ag nanoplates in Au-Ag plate heterostructures. (g) The statistics of the number of turns per Ag nanoplates in Au-Ag plate heterostructures in b. (h) The schematic illustration of the measurement of the length and width of Ag nanoplate in Au-Ag plate heterostructures.

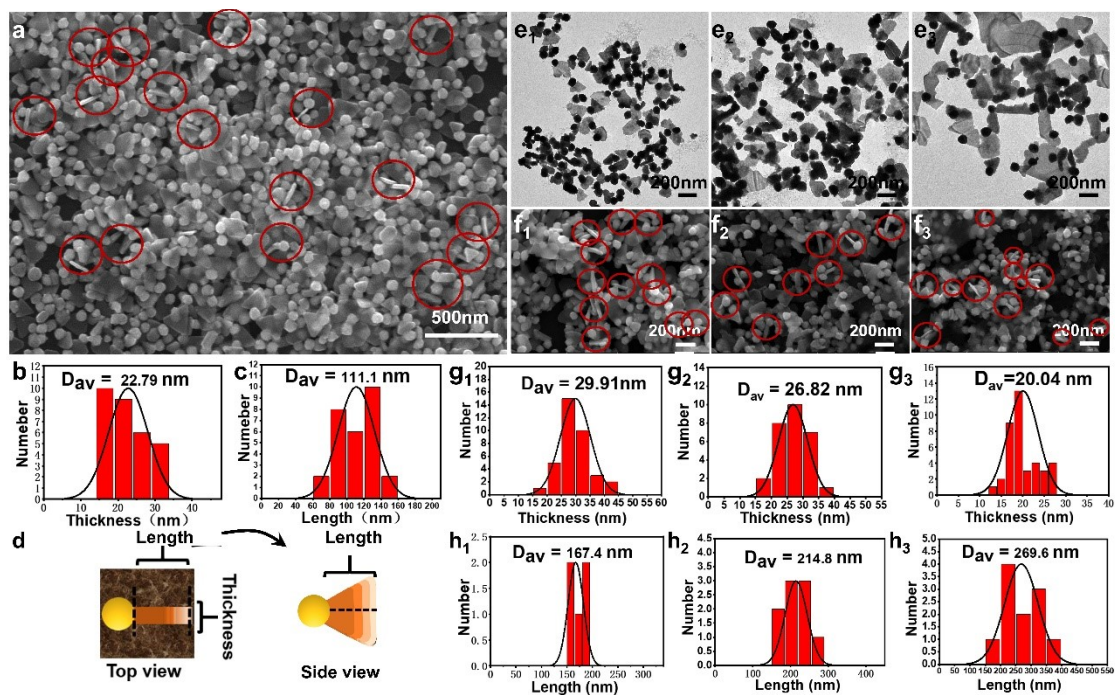


Fig. S5. (a) SEM image and the statistic distribution of the (b) thickness and (c) length of the Au-Ag triangle plate nanostructure. (d) The schematic illustration of the measured thickness and length of the Ag nanoplate in Au-Ag triangle plate heterostructures. (e) TEM images of the Au-Ag plate heterostructures synthesized at different concentration of MBIA ligand: (1) 0.10 mM; (2) 0.15 mM; (3) 0.20 mM. (f) SEM images with concentrated Au-Ag plate nanoparticles and the statistic average (g) thickness and (h) length of the Ag nanoplates in Au-Ag plate heterostructures.

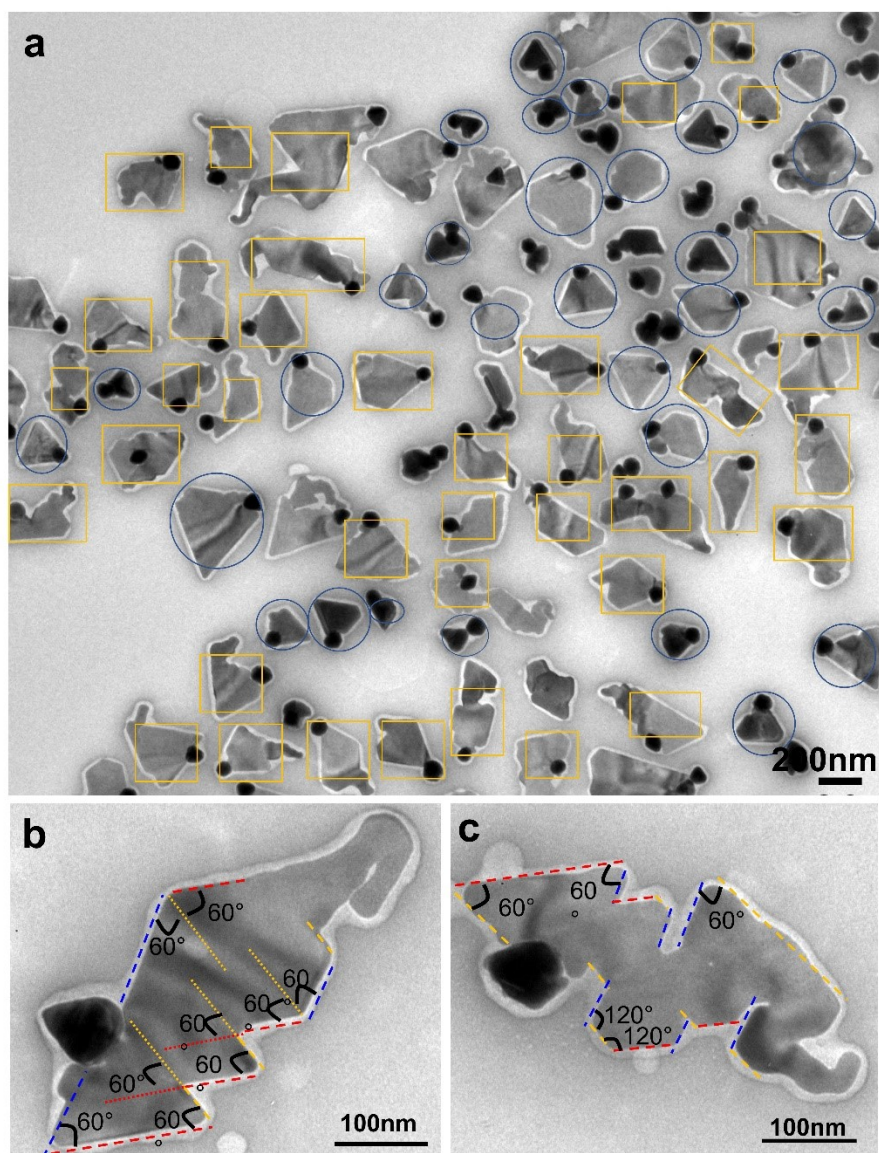


Fig. S6. (a) TEM image of Au-Ag plate hybrids in which the two types of structures were marked with circle (Type I) and square (Type II), respectively. (b-c) The enlarged TEM images of individual Au-Ag type II hybrid nanoparticles with marked angles in either 60 ° or 120 °.

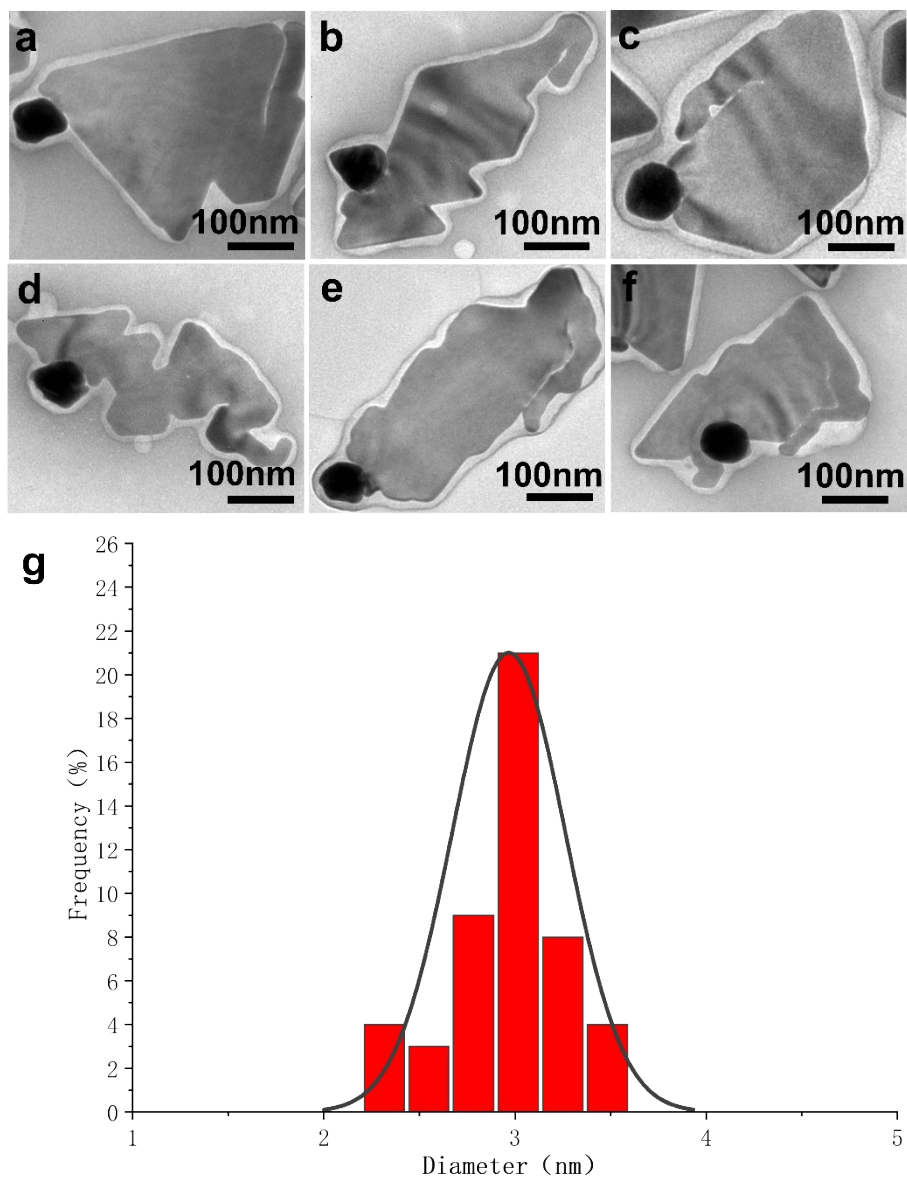


Fig. S7. (a-f) TEM image of Au-Ag plate hybrid structure and (g) gap diameter distribution.

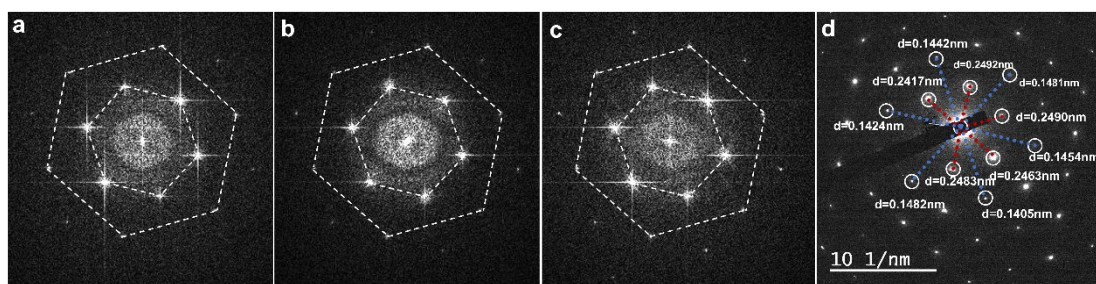


Fig. S8. (a-c) The diffraction patterns of the different area 1, 2, and 3 in Fig.3a in the maintext, in which the diffraction points were linked by dotted lines. These patterns can be completely overlapped, indicating their same lattice details. (d) The image is a measurement of the lattice spacing of selected area electron diffraction (SAED) in Fig. 3b.

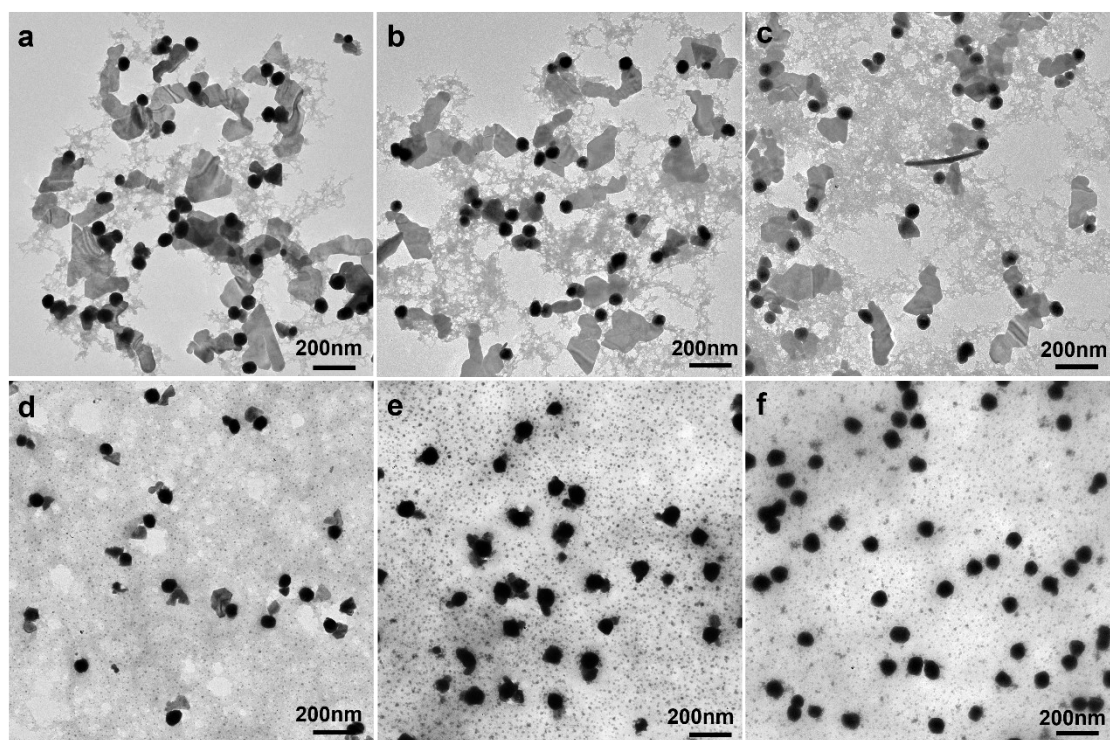


Fig. S9. The Au-Ag heterostructures synthesized under increased concentration of MBIA ligands: (a) 0.30, (b) 0.40, (c) 0.50, (d) 0.60, (e) 0.70 and (f) 0.80 mM.

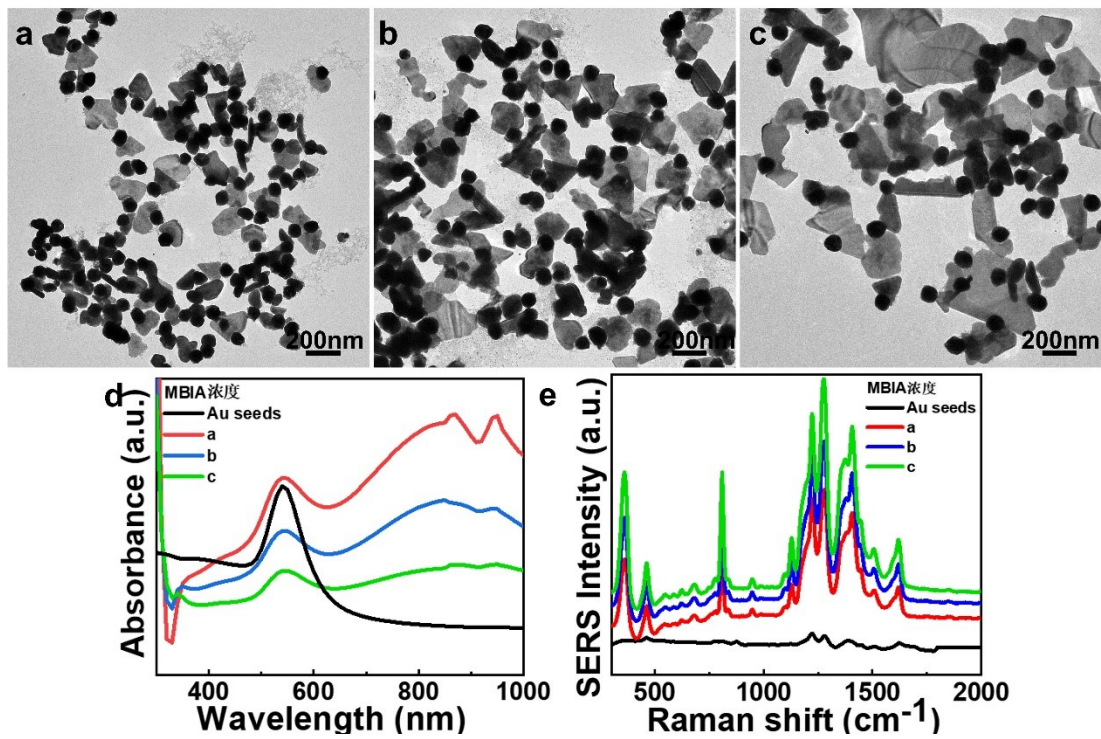


Fig. S10. (a-c) TEM images, (d) absorption spectra and (e) SERS of the Au seeds and the Au-Ag plate heterostructures synthesized by using different amounts of MBIA ligand: 0.10, 0.15 and 0.20 mM for a-c, respectively.

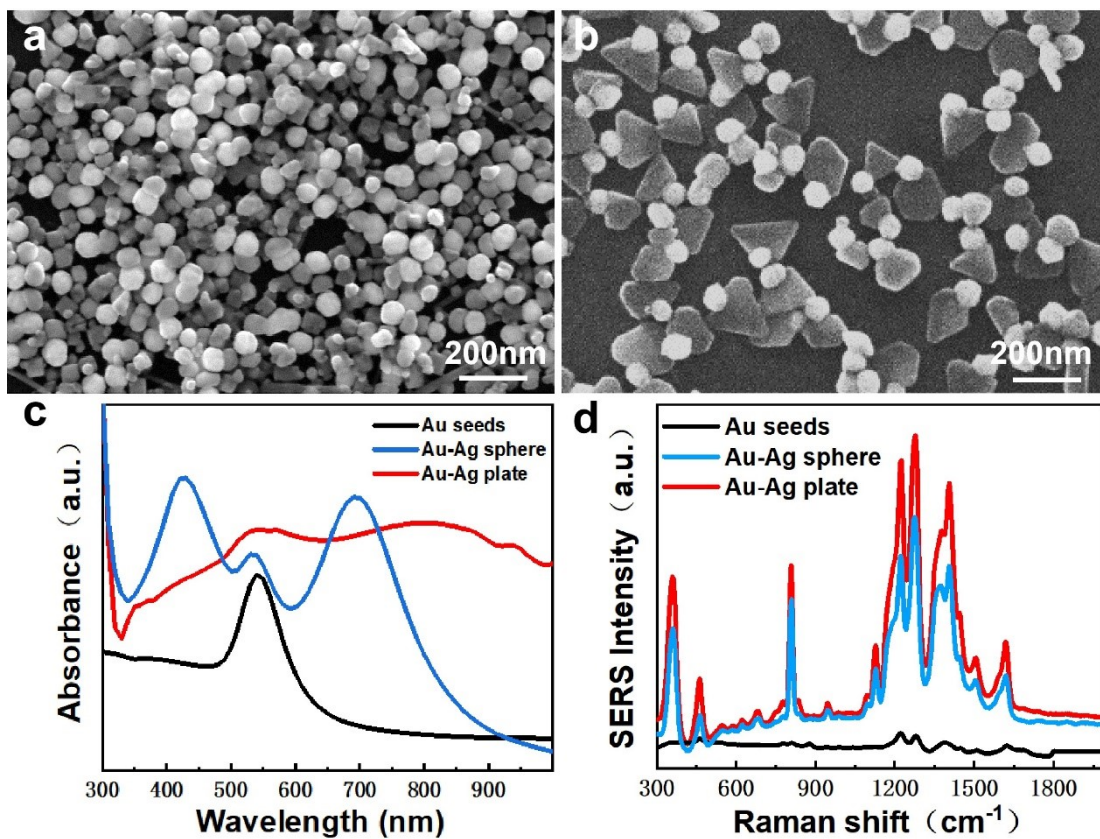


Fig. S11. SEM images of the (a) Au-Ag sphere and (b) Au-Ag triangle plate heterostructures. (c) UV-vis-NIR spectra and (d) SERS of the Au-Ag sphere and Au-Ag triangle plate heterostructures.

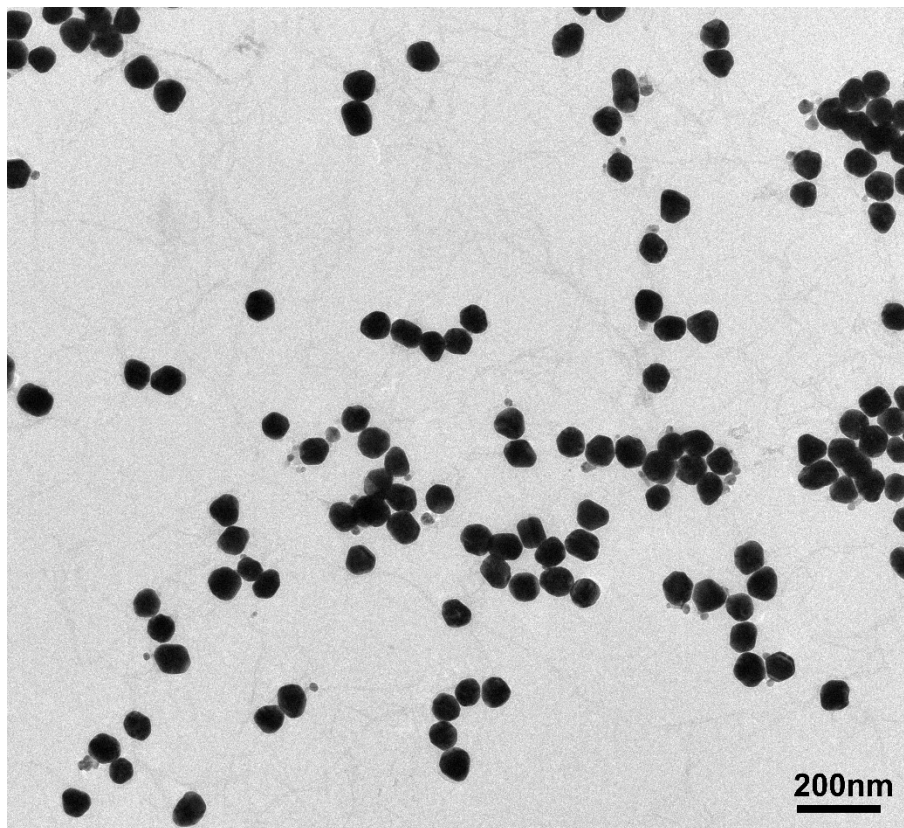


Fig. S12. TEM image of Au-Ag hybrid structure at low concentration of AgNO_3 and HQ (0.20 mM), used for the survey: small Ag nanoplate grown on some Au seeds about 26.53%.